American Mineralogist, Volume 97, pages 951–961, 2012

Determination of Fe^{3+}/Fe using the electron microprobe: A calibration for amphiboles

William M. Lamb,[1,*] Renald Guillemette,[1] Robert K. Popp,[1] Steven J. Fritz,[2,†] and Gregory J. Chmiel[2,‡]

[1]Department of Geology and Geophysics, Texas A&M University, College Station, Texas 77843-3115, U.S.A.
[2]Earth and Atmospheric Sciences Department, Purdue University, West Lafayette, Indiana 47907-2051, U.S.A.

Abstract

Iron is a common constituent in minerals from the Earth's crust and upper mantle and often occurs in minerals as mixtures of two valence states, Fe^{3+} or Fe^{2+}. Quantification of the values of Fe^{3+}/Fe_{Total}, where $Fe_{Total} = Fe^{3+}+Fe^{2+}$, in minerals may be necessary to accurately apply certain mineral equilibria to determine equilibrium values of important variables such as temperature (T), pressure (P), and oxygen fugacity (f_{O_2}). Most useful would be an analytical technique that permits determination of values of Fe^{3+}/Fe_{Total} within a single mineral grain that is contained within a standard petrographic thin section, and the excellent spatial resolution and relative accessibility of the electron microprobe (EMP) have resulted in various attempts to use this instrument to determine values of Fe^{3+}/Fe_{Total}. These efforts have typically involved quantifying characteristics of the Fe$L\alpha$ and/or Fe$L\beta$ peaks. In this paper, we employ the method of Fialin et al. (2001), who have shown that the location of the Fe$L\alpha$ peak changes as a function of Fe content and values of Fe^{3+}/Fe_{Total}, to determine values of Fe^{3+}/Fe_{Total} in amphiboles.

We have characterized the Fe$L\alpha$ peak in several amphiboles with known values of Fe^{3+}/Fe_{Total} using the electron microprobe at Texas A&M University. Initial analyses employed a beam current of 20 nA in an effort to avoid Fe-oxidation due to electron beam generated H-loss (Wagner et al. 2008). Subsequent analyses were conducted at 100 nA, and the results are consistent with the 20 nA data only when relatively short duration analytical times were used.

The position of the Fe$L\alpha$ peak was determined for three suites of amphiboles that have been experimentally treated such that grains in any one of these mineral suites are chemically identical except for differences in the values of Fe^{3+}/Fe_{Total}. A linear relation between the Fe$L\alpha$ peak location and value of Fe^{3+}/Fe_{Total} was observed for each of these three amphibole suites. These three lines differ from one another in both their slope and intercept and these differences vary as a function of Fe content. Thus, these amphiboles served as the basis for the derivation of a relation between Fe content and Fe$L\alpha$ peak location, both measured with the EMP, and the value of Fe^{3+}/Fe_{Total} as originally determined with ^{57}Fe Mössbauer spectroscopy. The relation between the relative peak position (RPP = hematite standard Fe$L\alpha$ peak position – amphibole Fe$L\alpha$ peak position), Fe content, and Fe^{3+}/Fe_{Total} is

$$Fe^{3+}/Fe_{Total} = RPP - RPP(0)/RPP(1) - RPP(0), \text{ where}$$
$$RPP(0) = -1.37 \times FeO^2 + 19.59 \times FeO - 3.85,$$
$$RPP(1) = -1.25 \times FeO^2 + 21.39 \times FeO + 13.05,$$

and FeO refers to the wt%FeO. This relation reproduces the measured values of Fe^{3+}/Fe_{Total} to within ±0.07 and, therefore, should permit determination values of Fe^{3+}/Fe_{Total} in amphiboles with Fe contents from 7 to 13 wt% FeO with similar precision. The amphiboles that were used in this study were kaersutites, Ti-bearing pargasites, and pargasitic hornblendes. The calibration presented here should, at the very least, be applicable to amphiboles with similar compositions, and although further verification is necessary, this calibration may be useful for determining values of Fe^{3+}/Fe_{Total} in amphiboles with distinctly different compositions and may even be more universally applicable.

Keywords: Amphibole, ferric-ferrous, electron microprobe, Fe oxidation state

Introduction

Iron is relatively common in rocks from the crust and upper mantle, and this element often occurs in more than one valence state. In general, application of mineral equilibria to quantify important parameters such as P, T, f_{O_2}, and f_{H_2} in the environment of mineral equilibration requires chemical characterization of the relevant phases and, in some cases, this characterization must include determination of Fe^{3+}/Fe_{Total}, where $Fe_{Total} = Fe^{3+} + Fe^{2+}$. For example, in a study of eclogites from Dabie Shan, E. China, Schmid et al. (2003) estimated peak temperatures that were ~80 to 100 °C higher than previous estimates that were based on the same geothermometers but

* E-mail: w-lamb@geos.tamu.edu
† Deceased
‡ Present address: Purdue Rare Isotope Measurement (PRIME) Laboratory, Department of Physics, Purdue University, West Lafayette, Indiana 47907-2036, U.S.A.

0003-004X/12/0506–951$05.00/DOI: http://dx.doi.org/10.2138/am.2012.3963

without information on the valence state of iron.

Values of f_{O_2} are typically inferred from mineral equilibria that involve a change in the oxidation state of Fe or other metal. Estimating values of f_{O_2} can provide important insight into the nature of fluids in the crust and upper mantle (Ague et al. 2001; Bryndzia and Wood 1990; Connolly and Cesare 1993; Creighton et al. 2009, 2010; Grant et al. 2007; Lamb and Valley 1985; Pawley et al. 1992; Simakov 2006; Wood et al. 1990; Wood and Virgo 1989; Woodland et al. 2006), and quantification of values of f_{O_2} often requires the determination of the valence state of Fe in one or more coexisting minerals.

The electron microprobe has become the standard analytical tool for the chemical characterization of minerals. This technique allows in situ analyses of minerals in thin section with a spatial resolution on the order of a few micrometers. However, conventional electron microprobe analyses do not routinely permit accurate determination of Fe^{3+}/Fe_{Total} in minerals. Thus, quantification of the valence state of Fe in minerals has typically involved application of other techniques, including: wet chemical analyses, ^{57}Fe Mössbauer spectroscopy, electron energy loss spectroscopy, X-ray photoelectron spectroscopy, and X-ray absorption spectroscopy (e.g., see McCammon 1999). Many of these methods require mineral separation and analysis of bulk samples. While the amount of sample required may be relatively small for some of these bulk techniques, examination in situ is often not possible and, therefore, it is impossible to detect zoning of Fe^{3+}/Fe_{Total} within a single grain. Where in situ analyses are possible (e.g., micro-XANES) rather specialized equipment is required.

Given the relatively good spatial resolution and accessibility of the electron microprobe, several attempts have been made to use this instrument to quantify values of Fe^{3+}/Fe_{Total} in various minerals. Although no information on Fe^{3+}/Fe_{Total} is directly available from conventional EMP analyses, it is sometimes possible to estimate values of Fe^{3+}/Fe_{Total} using known mineral stoichiometries by calculating the ratio of Fe^{3+} to Fe^{2+} that will result in a neutral charge for the mineral formula in question (i.e., charge balance). Procedures to estimate Fe^{3+}/Fe_{Total} based on charge balance have been widely applied in the petrologic literature (e.g., Droop 1987; Schumacher 1991), and estimates of Fe^{3+}/Fe_{Total} that are based on conventional EMP analyses are theoretically possible for anhydrous minerals that lack significant vacancies on any given crystallographic site (e.g., pyroxenes). However, even minerals that appear to be good candidates for estimates of Fe^{3+}/Fe_{Total} via charge balance may not be amenable to application of this technique due to inevitable uncertainties that arise when characterizing the chemical composition of minerals using the EMP. For example, Wood and Virgo (1989) show that conventional microprobe analyses of spinels from mantle lherzolites are sufficiently precise to determine values of Fe^{3+}/Fe_{Total}, yet systematic errors make this approach inaccurate unless spinels with independently determined values of Fe^{3+}/Fe_{Total} are used as secondary standards. Amphiboles are poor candidates for estimation of Fe^{3+}/Fe_{Total} by charge balance as they are hydrous, with possible substitution of O for OH on the O3 site, and they may have significant vacancies on the A-site (Hawthorne 1981).

Given the problems associated with determining values of Fe^{3+}/Fe_{Total} via charge balance, other methods have been developed to determine values of Fe^{3+}/Fe_{Total} with the EMP. These efforts typically involve quantifying some characteristic of the Fe$L\alpha$ peak or both Fe$L\alpha$ and $L\beta$ peaks. It has long been recognized that the location of these peaks and the value of $L\alpha$/$L\beta$ peak intensities vary with changes in the oxidation states of transition metals (Fischer 1965). More complete discussions of the theoretical basis for the relation between oxidation state of Fe and the characteristics of the Fe$L\alpha$ and Fe$L\beta$ are given in Armstrong (1999), Fialin et al. (2001, 2004), Höfer (2002), Höfer et al. (1994), and references therein.

Early efforts to use the EMP to quantify Fe^{3+}/Fe_{Total} in minerals were typically semi-quantitative, suffering from relatively large uncertainties (e.g., Albee and Chodos 1970; Dodd and Ribbe 1978; O'Nions and Smith 1971). Renewed interest in using the electron microprobe to determine Fe^{3+}/Fe_{Total} in minerals has produced more promising results. This more recent work has largely focused on two different approaches.

One of these two approaches continues to use the ratio of the $L\alpha$ to $L\beta$ peak intensities. However, rather than measure the area of these two peaks or the intensity at the wavelength of maximum intensity (i.e., the top of the peak), this method involves determining the intensities of the peaks at a position that is on the sides or the flanks of these peaks (Höfer et al. 1994). The flank method has been calibrated for, and used to, determine values of Fe^{3+}/Fe_{Total} in garnet (Creighton et al. 2009, 2010; Höfer and Brey 2007; Malaspina et al. 2010). Enders (2000) applied the flank method to sodic amphiboles and developed a calibration for these minerals that allows the determination of ferric/ferrous ratios to within an error of ±5% for sodic amphiboles with more than 6–8 wt% FeO.

A second method for determining values of Fe^{3+}/Fe_{Total} using the EMP is based on the energy of the Fe$L\alpha$ peak (Fialin et al. 2001, 2004). Peak energies can, of course, be related to the geometry of the EMP spectrometer via Bragg's law. In practice we describe peak energies in terms of the θ angle in Bragg's law and herein are reported in units of sine θ. Thus, we typically describe peak energies as peak locations and the location of Fe$L\alpha$ peak shifts as a function of certain variables, including the value of Fe^{3+}/Fe_{Total}. This shift is induced by self-absorption of the Fe X-ray and has, therefore, been termed the self-absorption-induced shift method (Fialin et al. 2001, 2004), although for the purposes of this paper we will use the phrase "peak-shift" method.

According to Fialin et al. (2004), the location of the Fe$L\alpha$ peak is not only dependent on the oxidation state of Fe, but it also depends on the total Fe concentration and, to a lesser extent, other characteristics of the bulk matrix. The peak-shift method, as used by Fialin et al. (2001, 2004), is calibrated by determining the location of the Fe$L\alpha$ peak as a function of Fe content. These peak locations are determined for two sets of minerals; in one set all Fe is Fe^{3+} and in the other set all Fe is Fe^{2+}. Thus, two end-member curves of peak position vs. Fe content have been produced (Fialin et al. 2001, 2004). Given these two curves, the value of Fe^{3+}/Fe_{Total} can be determined given the Fe content of a mineral, as determined from conventional EMP analyses, and the position of the Fe$L\alpha$ peak. This assumes that the change in peak location with Fe^{3+}/Fe_{Total} is linear between

the two end-member curves. Fialin et al. (2004) argue that this assumption is justified for glasses. This argument is supported by data depicted on Figure 4 of Fialin et al. (2004) that shows a linear relation between Fe$L\alpha$ peak position and independently determined values of Fe^{3+}/Fe_{Total}. However, for other minerals, such as garnets and Al-rich spinels, additional calibration may be required (Fialin et al. 2001).

Both the flank method and the peak-shift method require careful calibration using minerals of known Fe^{3+}/Fe_{Total}. The flank method may provide more rapid acquisition of the relevant data, as analyses are required on two points rather than a scan over an entire peak. This method does require careful spectrometer calibration, and Enders et al. (2000) argue that "...the flank method will probably not find use as a routine method." In spite of this cautionary statement, the flank method has been applied in several studies, particularly to the analyses of garnets, and its application may, therefore, become increasingly routine (Creighton et al. 2009, 2010; Malaspina et al. 2010).

Although the peak-shift method may be more time consuming than the flank method, the former method should be explored because it may be less sensitive than the flank method to chemical differences between standards and unknowns. The work of Fialin et al. (2001, 2004) indicates that the variation of the Fe$L\alpha$ peak position with Fe content for minerals with Fe as either all Fe^{3+} or all Fe^{2+} is independent of the type of mineral. For example, a plot of peak position vs. Fe content for various minerals in which all Fe is Fe^{2+} produces a smooth curve even though this plot was determined by making measurements on staurolite, clinopyroxene, orthopyroxene, and olivine (Fialin et al. 2001, their Fig. 3). Thus, it may be possible that a calibration based on minerals in which all the Fe is either Fe^{3+} or Fe^{2+} could be applied to a wide variety of minerals.

Another difference between the peak-shift and flank methods may be the precision that either method can ultimately achieve. Höfer et al. (1994) argue that application of the peak-shift method will generally involve an uncertainty of ±0.07, whereas the flank method may yield uncertainties of ±0.02. Höfer and Brey (2007) concluded that careful application of the flank method can yield uncertainties in Fe^{3+}/Fe_{Total} of ±0.02 in garnets. However, in the case of amphiboles, application of the flank method yielded a precision of ±5% (Enders et al. 2000), an uncertainty that is essentially identical to the uncertainty estimated by Fialin et al. (2004) for the peak-shift method.

This paper examines the use of the peak-shift method to determine values of Fe^{3+}/Fe_{Total} for amphiboles using the EMP. We have a suite of three amphiboles of known compositions, including values of Fe^{3+}/Fe_{Total} determined by ^{57}Fe Mössbauer spectroscopy or wet chemical analyses. The amphiboles were experimentally treated to provide a range of Fe^{3+}/Fe_{Total} from ~0 to 1.0 (Popp et al. 1995, 2006a, 2006b), and they provide an excellent opportunity to evaluate the applicability of the peak-shift method for determining Fe^{3+}/Fe_{Total} on this important mineral group. Our goal is to determine if, for any given Fe content, Fe$L\alpha$ peak locations determined for amphiboles shift in a linear fashion as a function of Fe^{3+}/Fe_{Total}. If so, then it should be possible derive a calibration based on these three amphiboles and assess the precision of the peak-shift technique when applied to these minerals.

EMP PROCEDURES AND ANALYTICAL CONDITIONS

Measurements were performed using a Cameca SX50 electron microprobe located in the Department of Geology and Geophysics at Texas A&M University using an accelerating voltage of 15 kV. Unless stated otherwise, the electron beam diameter was 20 μm, and the spectrometer pulse height analyzer (PHA) was set at a window width of 2000 mV to prevent potential higher order interferences from Fe and other elements in each sample.

Choice of beam current involves a trade-off between the desire to use higher beam currents and, therefore, shorter counting times, and the possibility of high beam currents resulting in changes in Fe^{3+}/Fe_{Total} of the amphiboles. We compare results obtained using two different beam currents, 20 nA and 100 nA. Our measurements were initiated prior to the publication of Wagner et al. (2008) whose results indicate that the electron beam can produce H-loss and simultaneous Fe-oxidation at beam currents of 240 and 100 nA and, in some cases, at currents as low as 50 nA. However, Wagner et al. (2008) observed that no changes in values of Fe^{3+}/Fe_{Total} were produced by a 10 nA beam current. Our own results are consistent with the use of a 20 nA beam current, and while 100 nA may sometimes produce H-loss in amphiboles (Wagner et al. 2008), our results at beam currents of 20 and 100 nA are largely self-consistent when counting times at 100 nA were reduced (as discussed more fully in subsequent sections of this paper).

A wavelength-dispersive spectrometer (WDS) containing a thallium acid phthalate (TAP) diffracting crystal was scanned over a range of sine θ centered on the Fe$L\alpha$ peak. Measurements used either 400 steps over a sine θ range of 0.02000 (2000×10^{-5} sine θ) or 200 steps over a range of 1000×10^{-5} sine θ. Count times per point were 200 ms, such that 80 s is required for measurements across 400 steps (40 s for 200 steps). A single measurement consisting of steps across the Fe$L\alpha$ peak will subsequently be referred to as a "scan."

A single scan did not result in sufficient counts to provide an acceptably low-noise peak shape that would permit accurate determination of the peak location, and so the results of several scans, typically ranging from 4 to 20, were accumulated. Thus, the time on a single 20 μm diameter area was typically on the order of 5.33 min (4 scans accumulated) to 26.67 min (20 scans accumulated). Even with these prolonged count times we typically analyzed more than one spot per sample. For example, with a beam current of 20 nA, on very high-Fe concentration samples such as hematite and magnetite, 10 scans on 5 different areas were typically accumulated, for a total count time of about 1.1 h. On minerals, such as amphibole, containing about 7–13 wt% FeO (recalculated total Fe), 20 scans of 400 steps on 10 to 20 different areas were typically accumulated, for a total count time of ~4.4 to 8.9 h. These long count times for amphibole were not only used to increase counting statistics, but also to analyze multiple grains in an effort to ensure we obtain a representative analyses of grains that might be slightly heterogeneous (see subsequent discussions for more details).

The peak locations were determined by fitting the X-ray intensity data to produce a smooth curve, and this curve was then used to determine the value of sine θ at the maximum intensity.

Various peak-fitting functions were investigated, including asymmetric versions of Gaussian, psuedo-Voight, and Pearson VII distributions. It is not clear that any particular function is, in all cases, superior to others in terms in the accuracy of the fit to the Fe$L\alpha$ peak. However, some functions, particularly symmetric functions, do not accurately describe many Fe$L\alpha$ peaks. In this study, we chose a fitting function that uses five different variables to describe peak characteristics. These variables are: (1) the peak location given as the sine θ value of the point on the peak that corresponds to the maximum intensity; (2) peak height or maximum intensity; (3) peak width at half height; (4) a factor to describe the distribution as either Gaussian and Lorenzian or some mixture of the two; and (5) an exponential "tail" factor, which is important for describing asymmetry. The function that uses these five variables is known as "ET" and is incorporated in a software package that is named "Plot[1]." Plot employs an iterative approach to find the appropriate solution, or fit, to the data, and it requires initial values, input by the user, for the five variables described above. The final fit to the data can depend upon these initial values and, therefore, it is important when relative comparisons of peak characteristics are made, as in this study, to input initial values in a consistent manner.

In summary, three different analytical conditions were used, all at an accelerating voltage of 15 kV. Analyses that were performed using a beam current of 20 nA used 400 steps over a range of 2000 × 10^{-5} sine θ. The times required for such an analysis varied depending on various factors including the number of amphibole grains used to obtain a single Fe$L\alpha$ peak. However, analytical times for amphiboles typically ranged from ~3.5 to 6.5 h for the analytical conditions of 20 nA and 400 steps. Analyses were also performed at 100 nA, initially over the same 400-step sine θ range. However, to reduce the time required, the sine θ range of subsequent peak characterizations at 100 nA was reduced by a factor of 2 such that 200 steps were used over a sine θ range of 0.01 (from 67 800 × 10^{-5} to 68 795 × 10^{-5} sine θ). In this case, with analytical conditions of 100 nA and 200 steps, counting times for amphiboles were often ~1 h when analyzing multiple grains. In subsequent sections of this paper, these different sine θ ranges are described by the number of steps involved in peak characterization (200 vs. 400 steps both using the same step size). However, the difference in the time the electron beam interacts with the sample is the variable of greatest importance to this study. All of the peak characteristics reported in this study where determined using data over the range 67 800 × 10^{-5} to 68 795 × 10^{-5} sine θ, even though in some cases, the data were originally collected over a wider sine θ range.

[1] "Plot" was written by Michael Wersemann and may be downloaded using the internet at the address http://plot.micw.eu/. Information available at this internet address includes documentation (that can also be obtained by contacting the first author) that contains a description of the function "ET."

Sample description, approach, and peak position reproducibility

Three of the amphiboles analyzed in this study have been experimentally treated hydrothermally and in air to produce samples of each that have constant Fe_{Total} but different values of Fe^{3+}/Fe_{Total}. One of these amphiboles is a titanian pargasite megacryst from Vulcan's Throne (VT), Arizona. The treatment and composition of this amphibole was described by Popp et al. (1995), and the composition is given in Table 1. Two additional amphiboles are described by Popp et al. (2006a, 2006b), one is a kaersutite from Greenland (GK) and the other is a titanian ferroan pargasitic hornblende from the Tschicoma Formation, New Mexico (TH). The compositions of these two amphiboles are tabulated in Table 1 (see also, Popp et al. 2006b). Samples of the three amphiboles are experimental run products that consist of tens to hundreds of grains with sizes ranging from ~10 to 20 μm up to 500 μm or more, as measured in the long dimension. Grains that were <25 μm across were too small to be used in this study, whereas larger grains were sometimes analyzed two to three times, although care was taken to avoid analyzing the same spot twice.

A fourth amphibole analyzed for this study is a natural pargasitic hornblende from Ontario, Canada (OPH). The composition of this amphibole is listed in Table 1, and the value of Fe^{3+}/Fe_{Total} is 0.44 as determined using the single dissolution wet chemical technique of Fritz and Popp (1985).

Two hematite samples were used in this study. One is a microprobe standard supplied by Charles M. Taylor whose characterization of this natural mineral indicates it is a stoichiometric hematite (99.95% pure). The second hematite sample, taken from a single crystal that originated in Brazil, was analyzed with the Texas A&M EMP. WDS analyses failed to detect Mg, Al, Si, Ti, Ca, and Mn, demonstrating that all of these elements must be present at levels less that 0.1 wt% of the oxide in question. The Fe$L\alpha$ peak was characterized for both of these hematite samples during a single analytical session. The average peak location for the Brazilian hematite was determined to be 68 314.9 ± 3.3 × 10^{-5} sine θ (number of analyses, n = 40) while the average peak location for the Taylor hematite was determined to be 68 312.1 ± 3.9 × 10^{-5} sine θ (n = 40). These EMP analyses demonstrate that there was no statistically significant difference in the Fe$L\alpha$ peak locations for these two hematite samples. Thus, these two standards were used interchangeably for this study.

Examples of Fe$L\alpha$ peak shapes for an amphibole, hematite, and magnetite are

Table 1. Amphibole compositions (wt% oxide with all Fe reported as FeO)

	Tschicoma hornblende			Vulcan's Throne				Greenland kaersutite	Ontario pargasitic hornblende	
	This study Average n = 269	St.dev.	Popp et al. (2006a) Average	This study Average n = 227	St.dev.	Popp et al. (1995) Average n = 210	St.dev.	Popp et al. (2006a)	This study Average n = 20	St.dev.
SiO_2	43.35	0.79	43.34	40.57	0.28	40.32	0.20	38.70	42.72	0.20
TiO_2	2.58	0.37	2.82	3.74	0.20	3.84	0.17	6.89	0.90	0.07
Al_2O_3	11.04	0.59	10.89	15.67	0.15	15.35	0.14	13.25	11.90	0.27
Cr_2O_3	0.02	0.03	0.01	0.03	0.02	BDL		BDL	0.01	0.02
MgO	13.58	0.56	13.93	14.53	0.18	14.53	0.14	13.19	14.41	0.19
CaO	11.06	0.22	11.11	10.42	0.65	10.46	0.14	12.48	11.59	0.07
MnO	0.22	0.04	0.21	0.08	0.03	BDL		0.11	0.29	0.03
FeO	12.34	0.67	13.13	7.42	0.19	7.70	0.18	10.10	10.96	0.28
Na_2O	2.06	0.11	2.13	2.68	0.08	2.74	0.05	2.52	2.62	0.09
K_2O	0.60	0.04	0.63	1.62	0.07	1.60	0.06	1.00	2.02	0.12
F	0.13	0.09	BDL	0.09	0.06	0.08	0.03	0.34	2.18	0.11
Cl	NA		BDL	NA		BDL		BDL	NA	
H_2O*	1.67		0.73	1.58	0.03	1.27		1.05	0.96	0.05
Total	98.65		98.93	98.43		97.89		99.63	100.56	

Note: BDL = below detection limits; NA = not analyzed.
* Measured (Popp et al.) or caclulated (this study), with calculated values based on mineral stoichimetry (Lamb and Popp 2009).

shown on Figure 1. Analyses that utilized 400 steps used over a range of 2000×10^{-5} sine θ typically captured the entire peak with measurements extending into the background regions on either side of the peak. Capturing the entire peak was one of the original goals of this study in an effort to determine which characteristics of the Fe$L\alpha$ peak changed as a function of Fe^{3+}/Fe_{Total}. We found that, in addition to the peak position, the peak height, width, and asymmetry (as measured by the "exponential tail" factor) all change systematically as the oxidation state of Fe changes. A complete discussion of these changes in peak characteristics is beyond the scope of this paper, however, preliminary analyses indicate that changes in peak position is at least as sensitive to changes in values of Fe^{3+}/Fe_{Total} as these other variables (e.g., peak width or asymmetry). To apply the peak-shift method, the peak position (sine θ value of the maximum intensity) must be determined with high precision, and, as discussed below, this is possible even when the sine θ range of data collection does not include the entire peak. Thus, analyses that used 200 steps over a range of 1000×10^{-5} sine θ were utilized even though these analyses did not capture the entire peak, particularly in the case of hematite (Fig. 1).

The Fe$L\alpha$ peak shape of hematite was characterized during each analytical session. This peak characterization served two purposes. First, Fe$L\alpha$ peak characteristics for a given sample may vary from one analytical session to the next, presumably due to small changes in temperature, atmospheric pressure, and other factors that can affect the mechanical and electronic components of the instrument. Thus, all peak positions are reported relative to the hematite peak such that the relative peak position (RPP) = hematite peak position – amphibole peak position. Second, the position of the hematite peak was measured periodically during any given analytical session to determine if drift occurred during the session. In most cases the Fe$L\alpha$ peak positions of hematite were determined after every one to three amphibole determinations, although, in one case, eight amphibole peaks were measured before a replicate hematite peak characterization. In no cases were systematic changes in hematite peak positions sufficiently large to warrant a correction for drift during a single analytical session, although significant changes in hematite peak positions sometimes occurred from one session to the next.

Replicate measurements on the hematite standard were used to determine the precision involved in Fe$L\alpha$ peak characterization. The analytical times were chosen to simulate the relatively low count rates of amphiboles with Fe contents that are much lower than that of hematite. The results are shown on Figure 2, which plots the number of counts at maximum peak height vs. the 1σ st.dev. of the mean peak location for values of n ranging from 4 to 40 (n = number of analyses). The results show no clear correlation between these two variables (Fig. 2). The average standard deviation is 3.0 ± 0.9 (1σ) for the values of maximum peak height depicted on Figure 2 (95 to 539 counts). For the purposes of this study we will use 3.0 ± 0.9 as an estimate of the precision of the measurements of Fe$L\alpha$ peak locations.

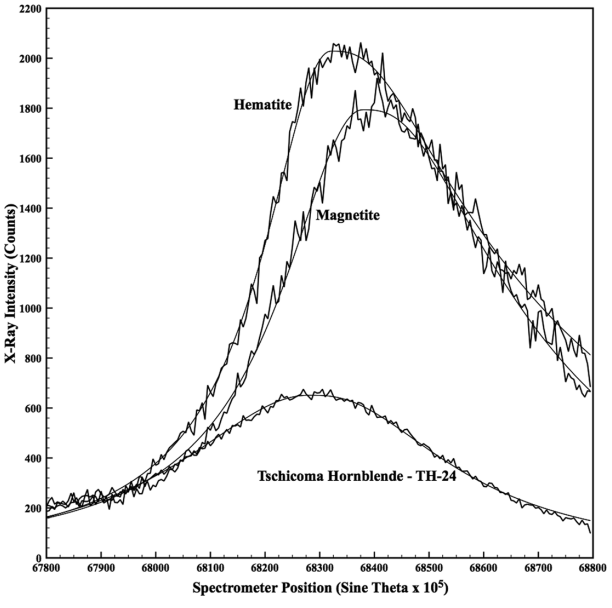

FIGURE 1. Examples of measured X-ray intensities plotted as a function of spectrometer position for three minerals. These data are fit by a curve that uses five variables to describe the peak (see text).

AMPHIBOLE PEAK SHIFT

Fe$L\alpha$ X-ray peak positions were determined for the 3 amphiboles with known values of Fe^{3+}/Fe_{Total} during different analytical sessions that occurred at different times and, in most cases, on different days. These values of Fe^{3+}/Fe_{Total} were determined on bulk samples via ^{57}Fe Mössbauer spectroscopy and, therefore, do not reflect zoning or grain-to-grain differences. Thus, in an effort to gather a representative data set, X-ray intensities were measured across the Fe$L\alpha$ peak on several grains and these intensities were combined to produce a single Fe$L\alpha$ peak. The Fe$L\alpha$ peak location is then based on a single fit to this combined data set. This approach was preferred over determining a peak location for each grain and then calculating an average because the relatively short counting times per grain did not produce an acceptably low noise peak. Certain analytical sessions were designed to replicate analyses on selected samples to evaluate the reproducibility of the technique and average values of peak positions have been determined only when replicate analyses have been performed.

The results from all analytical sessions are described below.

Tschicoma hornblende

Data were collected on 10 different samples of experimentally treated Tschicoma hornblende with values of Fe^{3+}/Fe_{Total} ranging from 0.11 to 0.95 (Table 2). In some cases replicate measurements were performed during different analytical sessions. At 20 nA (400 step scan) three of these replicate measurements were performed, whereas five replicate measurements were performed at 100 nA (200 step scan). The differences in the RPP for seven of these eight replicate measurements are $<4 \times 10^{-5}$ sine θ with one value of 9×10^{-5} sine θ (Table 2). These differences in the RPPs (Table 2) indicate that these measurements can be replicated to within the uncertainty estimate based on hematite Fe$L\alpha$ peak reproducibility. The Fe$L\alpha$ peak on hematite can be determined with a precision of $\pm 3.0 \times 10^{-5}$ sine θ (see previous

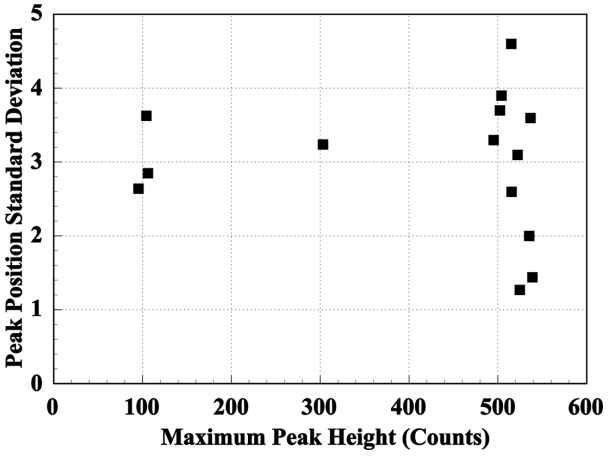

FIGURE 2. Average maximum peak height plotted against the 1σ st.dev. about the mean peak position (units are sine $\theta \times 10^5$) for replicate measurements performed on a hematite standard. The correlation between the two variables is weak and, therefore, the average 1σ st.dev. for all data points of 3.0 ± 0.9 (1σ) is taken as representative of the precision of peak position determinations (see text).

discussion). However, the RPP is based on the difference between two measurements and the combined uncertainty is 4.2×10^{-5} sine θ (e.g., see Appendix B in Williams 1987).

The results for the Tschicoma hornblende (Fig. 3) show a clear relation between the relative peak positions and Fe^{3+}/Fe_{Total}. For those samples in which relative peak positions were determined during more that one analytical session, the value plotted is an average of all sessions, and the error bar is the 1σ st.dev. about this average. Average peak positions for samples analyzed at 100 nA using a 200 step scan are often slightly larger that RPPs determined for peak positions determined at 20 nA, but these two data sets generally agree to within the precision estimated from replicated analyses on hematite ($\pm 4.2 \times 10^{-5}$ sine θ). Replicate analyses on the Tschicoma hornblende performed during different analytical sessions also typically agree within the expected analytical precision (Table 2). For low values of Fe^{3+}/Fe_{Total} (<0.45), peak positions determined using a combination of a high beam current (100 nA) and long counting time (400 step scan) are, in most cases, the largest values measured for any given sample.

Linear least-squares fits to the relative peak positions are plotted in Figure 3. In all cases the data are well represented by a straight line with R^2 values from 0.92 to 0.98. The linear fit to the data collected at 20 and 100 nA for relatively short durations (200 step scan) are offset, but they agree within uncertainty. The linear fit for data collected at 100 nA and 400 steps yields peak positions that are relatively large at low values of Fe^{3+}/Fe_{Total} ($Fe^{3+}/Fe_{Total} < \sim 0.6$), and, therefore, the slope of this line differs from linear fits determined for the two other analytical conditions (Fig. 3).

The differences in peak positions that were determined using different analytical conditions could be the result of H-diffusion generated by the heating of the amphibole by the electron beam (Wagner et al. 2008). In amphiboles, loss of hydrogen will result in an increase in Fe^{3+}/Fe_{Total} as illustrated by the following end-member reaction

$$Ca_2Fe_5^{2+}Si_8O_{22}(OH)_2 = Ca_2Fe_2^{3+}Fe_3^{2+}Si_8O_{22}(O)_2 + H_2. \quad (1)$$

Therefore, H-loss due to electron bombardment will result in an increase in the values of the relative peak position (Wagner et al. 2008). The potential for H-loss and, therefore, an increase in the RPP, is greatest at high-H contents (low Fe^{3+}/Fe_{Total}) and smallest at low-H contents (high Fe^{3+}/Fe_{Total}). No change in Fe$L\alpha$ peak positions due to H-diffusion is possible for samples in which all Fe is Fe^{3+}, because reaction 1 requires Fe^{2+} on the reactant side of the equation. Thus, all linear fits involving possible H-loss (oxidation) during the measurement would intersect at $Fe^{3+}/Fe_{Total} = 1$ and show the largest deviations at low Fe^{3+}/Fe_{Total}. Figure 3 indicates differences in RPPs are most pronounced for the conditions that combine relatively high beam currents and long analytical times (100 nA, 400 steps), particularly at low Fe^{3+}/Fe_{Total}, consistent with H-loss during analyses that combine the highest beam currents with the longest counting times. Consequently, data collected using a 100 nA beam current and 400 step scan were not used to determine the best-fit line for the relation between the RPP and Fe^{3+}/Fe_{Total}. However, relative peak positions for samples analyzed at the two other conditions (20 and 100 nA using a 200 step scan) generally agree to within

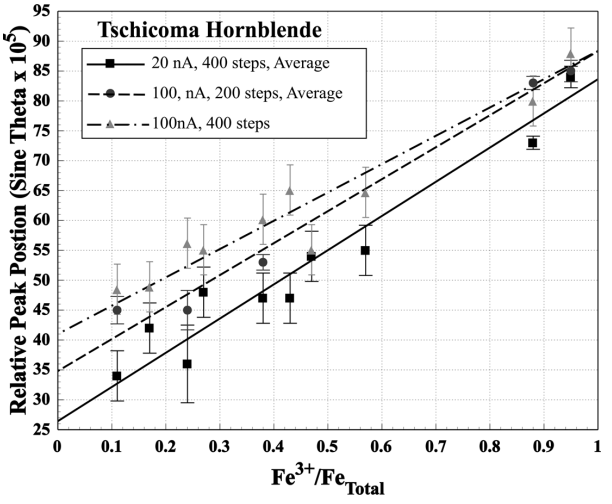

FIGURE 3. The relative peak positions (RPPs) for samples of the Tschicoma hornblende plotted against values of Fe^{3+}/Fe_{Total} as determined from ^{57}Fe Mössbauer spectroscopy. Error bars are either: (1) 1σ st.dev. values about the average value of the RPP calculated for those samples with replicate measurements from more than one analytical session, or (2) ±4.2 sine θ × 10^{-5} as estimated from reproducibility experiments on hematite (see text). Least-squares linear fits to the 20 nA, 400 step data (solid line: $R^2 = 0.94$); the 100 nA, 200 step data (long dashes: $R^2 = 0.98$); and the 100 nA, 400 step data (dash-dot: $R^2 = 0.92$) are shown.

TABLE 2. Relative peak positions (RPP) and maximum intensities for samples of the Tschicoma hornblende

		20 nA, 400 step scan								100 nA, 200 step scan								100 nA, 400 step scan		
		Session I			Session II					Session III			Session IV					Session V		
Sample	Fe^{3+}/Fe_{total}	RPP	Int*	Pts, Grns†	RPP	Int*	Pts, Grns†	Ave	Std Dev	RPP	Int*	Pts, Grns†	RPP	Int*	Pts, Grns†	Ave	Std Dev	RPP	Int*	Pts, Grns†
TH-11	0.11	34	180	1, 15						46	567	1, 10	43	565	1, 10	45	2.3	48	490	1, 7
TH-17	0.17	42	182	1, 15														49	572	1, 8
TH-24	0.24	36	181	1, 15	45	148	1, 13	41	6.5	43	651	1, 10	47	639	1, 10	45	3.3	56	571	1, 8
TH-27	0.27	48	180	1, 15														55	578	1, 8
TH-38	0.38	47	182	1, 15						53	655	1, 10	52	648	1, 10	53	1.3	60	492	1, 7
TH-43	0.43	47	182	1, 15														65	502	1, 7
TH-47	0.47	54	187	1, 15														55	502	1, 7
TH-57	0.57	55	184	1, 15														65	586	1, 8
TH-88	0.88	73	204	5, 3	71	190	1, 15	72	1.4	82	722	1, 10	84	717	1, 10	83	1.1	80	594	1, 8
TH-95	0.95	84	152	4, 2; 3, 1	81	193	1, 15	83	1.8	84	709	1, 10	87	711	1, 10	85	1.8	88	450	1, 6

* Int = Intensity.

† Pts = Points, Grns = Grains. Number of analytical spots per grain; Examples: (1) 1, 15 = 1 point on each of 15 grains, (2) 4, 2; 3, 1 = 4 points on each of 2 grains and 3 points on 1.

the expected precision ($\pm 4.2 \times 10^{-5}$ sine θ, see Table 2). This agreement argues against significant H-diffusion, as this would require that the analyses conducted using two different conditions coincidentally resulted in nearly identical changes in Fe^{3+}/Fe_{Total}.

The RPP determinations for sessions I through IV often involved analyses of different sets of grains. The precision of these RPP determinations (Table 2) indicates that grain-to-grain variation in Fe^{3+}/Fe_{Total} is not statistically significant at least when RPP values are based on averages of several grains.

Vulcan's Throne pargasite

Fourteen samples of the amphibole from Vulcan's Throne with different values of Fe^{3+}/Fe_{Total} were analyzed (Table 3). As was the case for the Tschicoma hornblende, these values of Fe^{3+}/Fe_{Total} were determined on bulk samples via ^{57}Fe Mössbauer spectroscopy. To determine the average peak position, we typically used the data collected on multiple grains, typically one spot on each grain (Table 3). In regard to the analytical procedures and number of grains analyzed, the following two points are noteworthy: (1) 60 different grains were analyzed on Sample VT-32 during session III, and (2) session IV consisted of analyzing 40 different grains on sample VT-07 with an electron beam diameter of 40 μm rather than the 20 μm diameter used for the other measurements.

Peak measurements made at 20 nA using data from 10 grains resulted in values of the maximum intensity that ranged from 69 to 88 counts (Table 3). These maximum intensities are slightly less than any of the values shown on Figure 2, yet most replicate analyses have a standard deviation in RPP that falls within the $\pm 4.2 \times 10^{-5}$ sine θ range.

As was the case for the Tschicoma hornblende, for those samples in which relative peak positions were determined during more that one analytical session, the value plotted is an average of all sessions, and the error bar is the 1σ st.dev. about this average (Fig. 4). For those samples where replicate analyses were not performed, the standard deviation is estimated to be $\pm 4.2 \times 10^{-5}$ as inferred from replicate analyses on hematite.

The relation between the relative peak position and values of Fe^{3+}/Fe_{Total} for samples of the Vulcan's Throne pargasite is linear with an R^2 value of 0.92 to 0.99 for least-squares best fits shown on Figure 4. The difference between the line that describes the data collected at 20 nA, and the line that describes the data collected at 100 nA using a relatively short counting time (200 step scan) is within $\pm 4.2 \times 10^{-5}$ sine θ. Therefore, as was the case for the Tschicoma hornblende, the data collected at these two analytical conditions are regarded as essentially equivalent. Data collected at 100 nA using longer counting times (400 step scan) typically yield the largest values for the relative peak position, and samples with values of $Fe^{3+}/Fe_{Total} < 0.4$ may have suffered from Fe oxidation due to H-loss produced by irradiation with the electron beam, as discussed above.

Greenland kaersutite

Results obtained on the Tschicoma hornblende and the Vulcan's Throne pargasite indicate that peak positions obtained using a beam current of 20 nA yield are essentially identical to those determined using a beam current of 100 nA using a 200 step scan. Thus, Fe$L\alpha$ peaks for the Greenland kaersutite have been characterized using only a beam current of 100 nA (200 step scan). Two sets of peak characterizations were performed using different 20 μm diameter areas on the same grains (Table 4). The results are depicted on Figure 5 and show the relation between values of the RPP and Fe^{3+}/Fe_{Total} that is well described by a straight line ($R^2 = 0.96$).

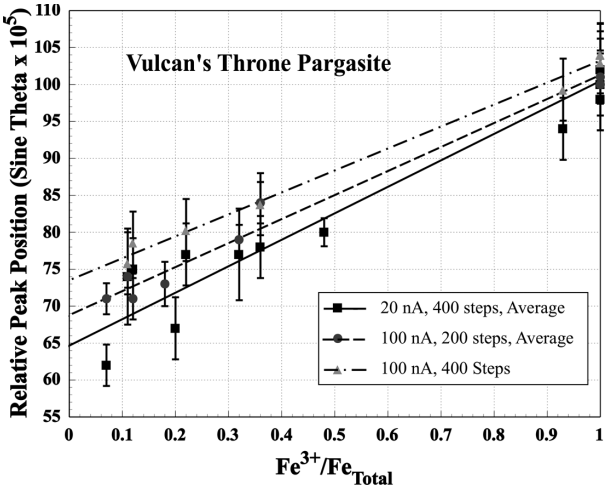

FIGURE 4. Relative peak positions (RPPs) for samples of the Vulcan's Throne pargasite plotted against Fe^{3+}/Fe_{Total} as determined from ^{57}Fe Mössbauer spectroscopy. Error bars are either: (1) 1σ st.dev. values about the average value of the RPP calculated for those samples with replicate measurements from more than one analytical session, or (2) ± 4.2 sine $\theta \times 10^{-5}$ (see text). Least-squares linear fits to the 20 nA, 400 step data (solid line: $R^2 = 0.92$); the 100 nA, 200 step data (long dashes: $R^2 = 0.98$); and the 100 nA, 400 step data (dash-dot: $R^2 = 0.99$) are shown.

A calibration based on three amphiboles

Each of the three amphiboles described in previous sections of this paper have different Fe contents (TH = 12.34%, GK = 10.10%, and VT = 7.42% with total Fe reported as wt% FeO), and experimentally treated samples of each amphibole have a range of different values of Fe^{3+}/Fe_{Total}. Given that the location of the Fe$L\alpha$ peak is largely a function of the two variables Fe content and Fe^{3+}/Fe_{Total} (Fialin et al. 2001, 2004), these three amphiboles provide the basis for a calibration that relates the relative Fe$L\alpha$ peak position, the Fe content, and the oxidation state of Fe. The relative Fe$L\alpha$ peak positions for the three amphiboles plotted vs. Fe^{3+}/Fe_{Total} are shown on Figure 5. In most cases, only those values of the RPP determined for data collected at 20 and 100 nA (200 step scans only) are used in constructing Figure 5 (Tables 2, 3, and 4). However, the RPPs determined for the samples of Vulcan's Throne hornblende in which values of Fe^{3+}/Fe_{Total} are 1.0 (samples VT-1A, VT-1B, and VT-1C, Table 3) are plotted even for RPPs that were determined using a 400 step scan at 100 nA. For these samples Fe^{3+}/Fe_{Total} is already at the maximum possible value and, therefore, no increase during electron bombardment through the operation of reaction 1 is possible.

The RPP variation for each amphibole plotted on Figure 5 is well described by a straight line (least-squares fit with R^2 values from 0.91 to 0.96). These linear fits were determined such that the x-axis (Fe^{3+}/Fe_{Total}) is a function of the y-axis (RPP),

TABLE 3. Relative peak positions (RPP) and maximum intenstities (Int) for samples of the Vulcan's Throne pargasite

		20 nA, 400 step scan													
		Session I			Session II			Session III			Session IV‡				
Sample	Fe^{3+}/Fe_{Total}	RPP	Int†	Pts, Grns*	RPP	Int†	Pts, Grns*	RPP	Int†	Pts, Grns*	RPP	Int†	Pts, Grns*	Ave	St.dev.
VT-07	0.07	65	72	1, 10	59	69	1, 10	60	126	1, 10	64	250	1, 40	62	2.8
VT-11	0.11	78	73	1, 10	69	73	1, 10							74	6.5
VT-12	0.12	75	142	1, 20										75	
VT-18	0.18														
VT-20	0.20				67	85	1, 12							67	
VT-22	0.22	77	74	1, 10										77	
VT-32	0.32				82	103	1, 15	73	382	1, 60				77	6.2
VT-36	0.36	78	74	1, 10										78	
VT-42	0.42	87	75	1, 10										87	
VT-48	0.48	79	76	1, 10	82	73	1, 10							80	1.9
VT-93	0.93	94	78	1, 10										94	
VT-1A	1.00	102	88	1, 10										102	
VT-1B	1.00	98	55	1, 7										98	
VT-1C	1.00	100	160	1, 20										100	

	100 nA, 200 step scan														100 nA, 400 step scan		
	Session V			Session VI			Session VII			Session VIII					Session IX		
Sample	RPP	Int†	Pts, Grns*	RPP	Int†	Pts, Grns*	RPP	Int†	Pts, Grns*	RPP	Int†	Pts, Grns*	Ave	St.dev.	RPP	Int†	Pts, Grns*
VT-07	73	419	1, 10	70	414	1, 10							71	2.1			
VT-11							73	416	1, 10	75	420	1, 10	74	1.5	76	537	1, 12
VT-12	69	431	1, 10	73	420	1, 10							71	2.8	79	536	1, 12
VT-18	75	431	1, 10	71	435	1, 10							73	3.0			
VT-20																	
VT-22															80	542	1, 12
VT-32	78	423	1, 10	80	418	1, 10							79	2.0			
VT-36	86	432	1, 10	82	438	1, 10							84	2.8	84	543	1, 12
VT-42															93	546	1, 12
VT-48																	
VT-93															99	556	1, 12
VT-1A															104	565	1, 12
VT-1B							96	437	1, 10	105	445	1, 10	100	6.2	104	561	1, 12

* Pts = Points, Grns = Grains. Number of analytical spots per grain; for example 1, 10 = one point on each of 10 grains.
† Int = intensity.
‡ Session IV: 40 µm spot size.

and, therefore, the slopes of these three lines are negative. The values of these slopes range from –1.8 (VT), to –1.2 (GK), and finally to –0.5 (TH) suggesting that the slopes of these three lines increase with increasing FeO content. This result is consistent with previous application of the peak-shift method as shown by Figure 3 of Fialin et al. (2001) and Figure 2 of Fialin et al. (2004). Both of these figures indicate that the difference in the Fe$L\alpha$ peak positions between minerals in which all Fe is divalent and minerals in which all Fe is trivalent increases with increasing Fe content. If values of Fe^{3+}/Fe_{Total} change in a linear fashion between these two end-member curves (an assumption consistent with the analyses of the amphiboles examined in this study), then plotting Fe^{3+}/Fe_{Total} vs. the Fe$L\alpha$ peak position (as shown on Fig. 5), should result in a series of straight lines that exhibit increasing slope with increasing FeO content. Thus, the results depicted on Figure 5 are qualitatively consistent with the results of Fialin et al. (2001, 2004).

Fialin et al. (2001, 2004) determined two best-fit curves for data relating peak positions and Fe content, one curve for minerals with $Fe^{3+}/Fe_{Total} = 0$ and another curve for minerals with $Fe^{3+}/Fe_{Total} = 1.0$. If, at any given Fe content, the oxidation state of Fe and the Fe$L\alpha$ peak positions are linearly related then values of Fe^{3+}/Fe_{Total} can be determined from the location of the Fe$L\alpha$ peak in question relative to these two "end-member" curves. We have adopted this approach to determine a calibration based on the RPP data for the three amphiboles studied here.

The intercepts of the three lines on Figure 5 on the y-axis where $Fe^{3+}/Fe_{Total} = 0$ yield values of the RPP of 66, 54, and 29 for FeO contents of 7.42, 10.1, and 12.34 wt%, respectively. A second-order polynomial was fit to these three data points, yielding

$$RPP(0) = -1.37 \times FeO^2 + 19.59 \times FeO - 3.85 \quad (2)$$

where RPP(0) is the relative peak position at $Fe^{3+}/Fe_{Total} = 0$ and FeO refers to the wt% FeO. Similarly, the intercepts of the three lines on Figure 5 on the y-axis where $Fe^{3+}/Fe_{Total} = 1$ yield three values of the RPP of 103, 101, and 86 for FeO contents of 7.42, 10.1, and 12.34 wt%, respectively. A second-order polynomial was fit to these three data points, yielding

$$RPP(1) = -1.25 \times FeO^2 + 21.39 \times FeO + 13.05 \quad (3)$$

where RPP(1) is the relative peak position at $Fe^{3+}/Fe_{Total} = 1$. For any given Fe content, if values of Fe^{3+}/Fe_{Total} in amphiboles vary in a linear manner between the curves given by Equations 2 and 3, then the relation between RPP, Fe content, and Fe^{3+}/Fe_{Total} is

$$Fe^{3+}/Fe_{Total} = RPP - RPP(0)/RPP(1) - RPP(0) \quad (4)$$

where RPP is the measured relative peak positions of the mineral in question and RPP(0) and RPP(1) are calculated using

TABLE 4. Relative peak positions (RPP) and maximum intenstities for samples of the Greenland kaersutite

		100 nA, 200 step scan							
		Session I			Session II				
Sample	Fe^{3+}/Fe_{Total}	RPP	Int*	Pts, Grns†	RPP	Int*	Pts, Grns†	Ave	St.dev.
GK-13	0.13	60	453	1, 10	59	462	1, 10	60	0.4
GK-24	0.24	70	344	1, 8	67	456	1, 10	68	1.6
GK-34	0.34	67	405	1, 9	69	452	1, 10	68	1.3
GK-44	0.44	76	360	1, 8	74	366	1, 8	75	1.5
GK-51	0.51	79	332	1, 7	74	328	1, 7	77	3.5
GK-79	0.79	91	414	1, 9	90	422	1, 9	91	1.1

* Int = Intensity.
† Pts = Points, Grns = Grains. Number of analytical spots per grain; for example 1, 10 = one point on each of 10 grains.

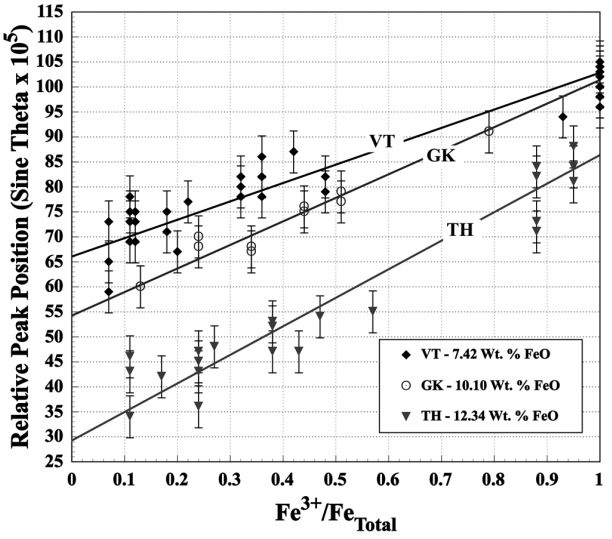

FIGURE 5. The relative peak positions (RPPs) for samples of the three different amphiboles plotted against Fe^{3+}/Fe_{Total} as determined from ^{57}Fe Mössbauer spectroscopy. In contrast to Figures 3 and 4, average values from different analytical session are not shown. Rather all data from each analytical session are plotted. Error bars are $\pm 4.2 \sin\theta \times 10^{-5}$ as estimated from reproducibility experiments on hematite (see text). Linear least-squares fits to the TH ($R^2 = 0.93$), VT ($R^2 = 0.91$), and the GK ($R^2 = 0.96$) RPP data are shown.

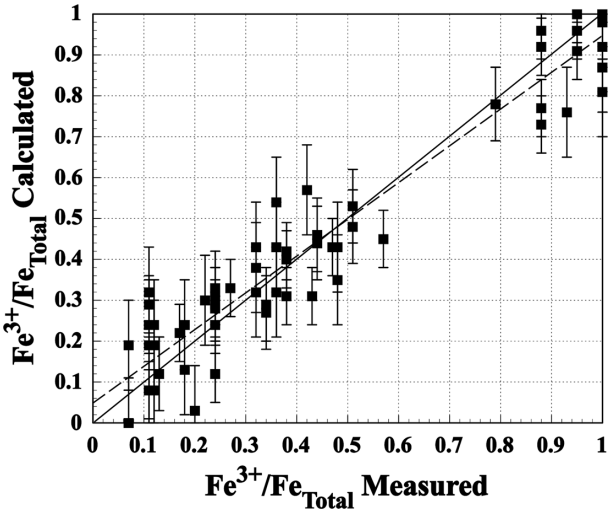

FIGURE 6. A comparison between values of Fe^{3+}/Fe_{Total} measured using ^{57}Fe Mössbauer spectroscopy vs. values of Fe^{3+}/Fe_{Total} calculated with Equation 4. The solid line represent perfect, or one-to-one, correspondence, whereas the dashed line is a linear least-squares fit to the data.

Equations 2 and 3, respectively. As a check on the consistency of Equation 4 in predicting Fe^{3+}/Fe_{Total}, the equation was used to calculate the values of Fe^{3+}/Fe_{Total} from the experimentally measured values of RPP reported in Tables 2, 3, and 4. The calculated values of Fe^{3+}/Fe_{Total} are plotted against values of Fe^{3+}/Fe_{Total} determined using ^{57}Fe Mössbauer spectroscopy (Fig. 6). The average of the absolute values of the difference between the calculated and measured (i.e., calculated-observed) is 0.07.

Equation 4 was used to construct the contours of constant wt% FeO on the plot of RPP vs. Fe^{3+}/Fe_{Total} shown in Figure 7. Also plotted on Figure 7 are the values for the natural pargasitic hornblende from Ontario, Canada (OPH, Table 1), at RPP = 73 and 10.96 wt% FeO, obtained using the Texas A&M University electron microprobe. Based on Equation 4, a value for Fe^{3+}/Fe_{Total} of 0.54 is obtained for the hornblende. This value is slightly larger than, but favorably comparable to, the value of 0.44 that was determined for the OPH using the wet chemical technique of Fritz and Popp (1985).

DISCUSSION

The calibration presented here, based on three suites of experimentally treated amphiboles, reproduces the measured values of Fe^{3+}/Fe_{Total} to within ± 0.07 (1σ). The experimental treatment of amphiboles produced a relatively large number of samples with Fe^{3+}/Fe_{Total} that are less than ~0.6, and fewer samples with more elevated values of Fe^{3+}/Fe_{Total} (Fig. 5). As described more fully in Popp et al. (1995, 2006a, 2006b) the more elevated values of Fe^{3+}/Fe_{Total} result from heating the amphiboles in air, while hydrothermal treatment, even under the relatively oxidizing conditions of the hematite-magnetite oxygen buffer, generally resulted in amphiboles with lower values of Fe^{3+}/Fe_{Total} (typically <0.6). Given this relative shortage of highly oxidized samples we have taken particular care to replicate analyses using amphiboles with $Fe^{3+}/Fe_{Total} > 0.6$. Thus, for the Vulcan's Throne amphibole, 11 determinations of the Fe$L\alpha$ peak position were conducted on samples with Fe^{3+}/Fe_{Total} of 0.93 or greater, with each determination based on several amphiboles (Table 3). Similarly, eight Fe$L\alpha$ peak location determinations were conducted on samples of the Tschicoma hornblende with Fe^{3+}/Fe_{Total} of 0.88 or greater, again with each determination based on several amphiboles (Table 2).

However, no samples of the Greenland kaersutite have a value Fe^{3+}/Fe_{Total} greater than 0.79 and only one sample has Fe^{3+}/Fe_{Total} greater than 0.51 (Table 4). Thus, the slope of the best-fit line for the GK is not as well constrained as the slopes for the TH and VT amphibole.

Given the empirical nature of this calibration, additional verification would be warranted for amphiboles with Fe contents that differ significantly from the amphiboles used in our calibration (i.e., wt% FeO >7 and <13). Furthermore, all amphiboles used in this calibration were Al-rich calcic amphiboles with significant Na and variable amounts of Ti (i.e., kaersutite, pargasite, and pargasitic hornblende). This calibration may be applied to other amphiboles with similar chemical characteristics and is particularly well suited for most amphiboles that have formed in the Earth's mantle. However, without additional testing, caution should be exercised when dealing with amphiboles whose crystal chemistry differs significantly from those examined in this study (e.g., orthoamphiboles and Al-poor calcic amphiboles).

Equation 4 recreates the Fe$L\alpha$ peak location data used in the calibration with a 1σ precision of ±0.07, which is equivalent to the precision of the peak-shift method estimated by Höfer et al. (1994). However, the precision of Fe^{3+}/Fe_{Total} determinations should improve with increasing Fe content. For example, an uncertainty in peak location of $\pm 4.2 \times 10^{-5}$ sine θ, when evaluated using Equation 4, yields an uncertainty of ±0.12 for an FeO content of 7 wt%, and ±0.07 for an FeO content of 13 wt%. Furthermore, amphibole analyses require relatively low sample currents and restricted counting times to avoid electron beam induced H-loss and simultaneous oxidation of Fe. Anhydrous phases may prove to be more robust and, therefore, significantly higher beam currents and/or counting times may yield sufficient count rates to increase the precision of Fe$L\alpha$ peak location determinations. Thus, the peak-shift technique may prove to be more precise when applied to anhydrous phases as opposed to amphiboles, or other hydrous phases. Furthermore, the characteristics of the Fe$L\alpha$ X-ray peak were measured over two different ranges of sine θ (0.01 and 0.02) and both yielded a consistent relation between Fe$L\alpha$ X-ray energies, Fe content, and Fe^{3+}/Fe_{Total}, even though the more narrow scan range may result in the truncation of some portion of the peak. It may, therefore, be possible to further narrow the range of sine θ over which X-ray intensities are measured. This would permit either larger values of the X-ray peak height for the same counting times, or shorter amounts of time required for peak characterization. Increasing X-ray peak heights might increase analytical precision, whereas shorter analytical times would make these measurements more convenient and further guard against significant changes in Fe^{3+}/Fe_{Total} due to H-diffusion induced by interaction of an amphibole with the electron beam.

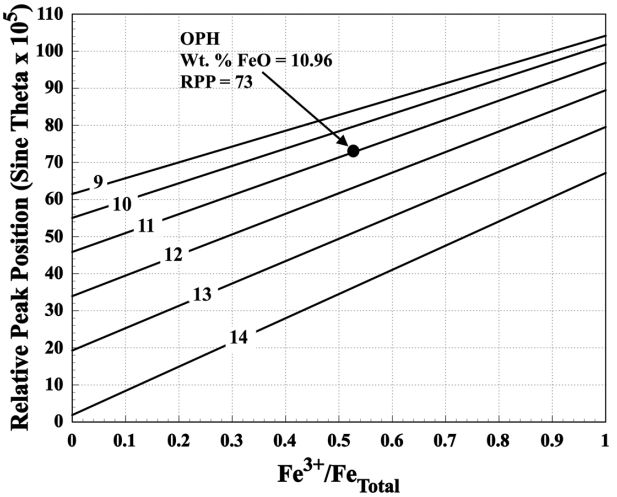

FIGURE 7. The relations between RPP and Fe^{3+}/Fe_{Total} are shown for Fe contents ranging from 9 to 14 wt% FeO. Locations of the lines were calculated using Equation 4.

The estimated precision of our calibration (±0.07) is sufficient for the application to many geologic problems involving amphibole equilibria. For example, Lamb and Popp (2009) used a dehydrogenation equilibrium (Eq. 1) to estimate a value of the hydrogen fugacity for an amphibole-bearing sample from the earth's mantle. This estimate of f_{H_2} was combined with an estimate of the oxygen fugacity for the sample to determine a value of the activity of H_2O (a_{H_2O}). The estimated value of f_{H_2} was based on the composition of a mantle amphibole, including a value of $Fe^{3+}/Fe_{Total} = 0.90$ determined by ^{57}Fe Mössbauer spectroscopy, and yielded a value of $a_{H_2O} = 5 \times 10^{-4}$. Propagating an assumed uncertainty of ±0.07 through the calculation of a_{H_2O} produces the following: if Fe^{3+}/Fe_{Total} were 0.83 then $a_{H_2O} \approx 2 \times 10^{-3}$, whereas a Fe^{3+}/Fe_{Total} of 0.97 yields $a_{H_2O} \approx 1 \times 10^{-4}$. In all cases values of a_{H_2O} are low and are within approximately one order of magnitude. Thus, measurement of Fe^{3+}/Fe_{Total} using the calibration described here would be useful in this case, and could also provide insight into spatial variations in values of Fe^{3+}/Fe_{Total} within sufficiently large single crystals.

Fialin et al. (2004) have examined the Fe$L\alpha$ peak energies as a function of Fe content and Fe^{3+}/Fe_{Total} and have produced a calibration based on minerals in which the Fe is either entirely Fe^{2+} or all Fe^{3+} to determine the values of Fe^{3+}/Fe_{Total} in glasses. Previous work (e.g., Fialin et al. 2001) suggests that this same approach could be applied to other minerals, including garnets and Al-rich spinels, although this approach may require additional calibration. Future work could focus on improving the precision of these analyses and extending this calibration to encompass a wider range of amphibole compositions and perhaps even phases other than amphibole. A refined calibration could also be tested against other micro-analytical methods, including the flank method (e.g., Höfer and Brey 2007), which have been used to determine Fe^{3+}/Fe_{Total} in minerals.

ACKNOWLEDGMENTS

We thank Christiane Wagner and Heidi Hoefer for their careful reviews of an earlier version of this manuscript. We dedicate this paper to our friend and colleague Steve Fritz, who passed away on the 21st of June 2008.

REFERENCES CITED

Ague, J.J., Baxter, E.F., and Eckert, J.O. (2001) High fO_2 during sillimanite zone metamorphism of part of the Barrovian type locality, Glen Clova, Scotland. Journal of Petrology, 42, 1301–1320.

Albee, A.L. and Chodos, A.A. (1970) Semiquantitative electron microprobe determination of Fe^{2+}/Fe^{3+} and Mn^{2+}/Mn^{3+} in oxides and silicates and its application to petrologic problems. American Mineralogist, 55, 491–501.

Armstrong, J.T. (1999) Determination of chemical valence state by X-ray emission analysis using electron beam instruments: Pitfalls and promises. Analytical

Chemistry, 71, 2714–2724.
Bryndzia, L.T. and Wood, B.J. (1990) Oxygen thermobarometry of abyssal spinel peridotites—the redox state and C-O-H volatile composition of the earth's sub-oceanic upper mantle. American Journal of Science, 290, 1093–1116.
Connolly, J.A.D. and Cesare, B. (1993) C-O-H-S fluid composition and oxygen fugacity in graphitic metapelites. Journal of Metamorphic Geology, 11, 379–388.
Creighton, S., Stachel, T., Matveev, S., Hofer, H., McCammon, C., and Luth, R.W. (2009) Oxidation of the Kaapvaal lithospheric mantle driven by metasomatism. Contributions to Mineralogy and Petrology, 157, 491–504.
Creighton, S., Stachel, T., Eichenberg, D., and Luth, R.W. (2010) Oxidation state of the lithospheric mantle beneath Diavik diamond mine, central Slave craton, NWT, Canada. Contributions to Mineralogy and Petrology, 159, 645–657.
Dodd, C.G. and Ribbe, P.H. (1978) Soft-X-ray spectroscopy of ferrous silicates. Physics and Chemistry of Minerals, 3, 145–162.
Droop, G.T.R. (1987) A general equation for estimating Fe^{3+} concentrations in ferromagnesian silicates and oxides from microprobe analyses using stoichiometric criteria. Mineralogical Magazine, 51, 431–435.
Enders, M., Speer, D., Maresch, W.V., and McCammon, C.A. (2000) Ferric/ferrous iron ratios in sodic amphiboles: Mössbauer analysis, stoichiometry-based model calculations and the high-resolution microanalytical flank method. Contributions to Mineralogy and Petrology, 140, 135–147.
Fialin, M., Wagner, C., Metrich, N., Humler, E., Galoisy, L., and Bezos, A. (2001) $Fe^{3+}/\Sigma Fe$ vs. Fe$L\alpha$ peak energy for minerals and glasses: Recent advances with the electron microprobe. American Mineralogist, 86, 456–465.
Fialin, M., Bezos, A., Wagner, C., Magnien, V., and Humler, E. (2004) Quantitative electron microprobe analysis of $Fe^{3+}/\Sigma Fe$: Basic concepts and experimental protocol for glasses. American Mineralogist, 89, 654–662.
Fischer, D.W. (1965) Changes in soft X-ray L emission spectra with oxidation of first series transition metals. Journal of Applied Physics, 36, 2048–2053.
Fritz, S.F. and Popp, R.K. (1985) A single-dissolution technique for determining FeO and Fe_2O_3 in rock and mineral samples. American Mineralogist, 70, 961–968.
Grant, K.J., Brooker, R.A., Kohn, S.C., and Wood, B.J. (2007) The effect of oxygen fugacity on hydroxyl concentrations and speciation in olivine: Implications for water solubility in the upper mantle. Earth and Planetary Science Letters, 261, 217–229.
Hawthorne, F.C. (1981) Crystal chemistry of the amphiboles. In D.R. Veblen, Ed., Amphiboles and Other Hydrous Pyriboles—Mineralogy, 9A, p. 1–102. Reviews in Mineralogy, Mineralogical Society of America, Chantilly, Virginia.
Höfer, H.E. (2002) Quantification of Fe^{2+}/Fe^{3+} by electron microprobe analysis—New developments. Hyperfine Interactions, 144, 239–248.
Höfer, H.E. and Brey, G.P. (2007) The iron oxidation state of garnet by electron microprobe: Its determination with the flank method combined with major-element analysis. American Mineralogist, 92, 873–885.
Höfer, H.E., Brey, G.P., Schulzdobrick, B., and Oberhansli, R. (1994) The determination of the oxidation-state of iron by the electron-microprobe. European Journal of Mineralogy, 6, 407–418.
Lamb, W.M. and Popp, R.K. (2009) Amphibole equilibria in mantle rocks: Determining values of mantle a_{H_2O} and implications for mantle H_2O contents. American Mineralogist, 94, 41–52.
Lamb, W.M. and Valley, J.W. (1985) C-O-H fluid calculations and granulite genesis. In A. Tobi and J. Touret, Eds., The Deep Proterozoic Crust in the North Atlantic Provinces, p. 119−131. Reidel, Dordrecht.
Malaspina, N., Scambelluri, M., Poli, S., Van Roermund, H.L.M., and Langenhorst, F. (2010) The oxidation state of mantle wedge majoritic garnet websterites metasomatised by C-bearing subduction fluids. Earth and Planetary Science Letters, 298, 417–426.
McCammon, C.A. (1999) Methods for determination of $Fe^{3+}/\Sigma Fe$ in microscopic samples. In J.J. Gurney, J.L. Gurney, M.D. Pascoe, and S.H. Richardson, Eds., Proceedings of the International Kimberlite Conference, 7, p. 540–544. Red Roof Design, Cape Town, South Africa.
O'Nions, R.K. and Smith, D.G.W. (1971) Investigations of the $L_{II,III}$ X-ray emission spectra of Fe by electron microprobe. Part 2. Fe $L_{II,III}$ spectra of Fe and Fe-Ti oxides. American Mineralogist, 56, 1452–1463.
Pawley, A.R., Holloway, J.R., and McMillan, P.F. (1992) The effect of oxygen fugacity on the solubility of carbon-oxygen fluids in basaltic melt. Earth and Planetary Science Letters, 110, 213–225.
Popp, R.K., Virgo, D., Yoder, H.S., Hoering, T.C., and Phillips, M.W. (1995) An experimental study of phase equilibria and Fe oxy-component in kaersutitic amphibole: Implications for the f_{H_2} and a_{H_2O} in the upper mantle. American Mineralogist, 80, 534–548.
Popp, R.K., Hibbert, H.A., and Lamb, W.M. (2006a) Erratum: Oxy-amphibole equilibria in Ti-bearing calcic amphiboles: Experimental investigation and petrologic implications for mantle-derived amphiboles (vol 91, pg 54, 2006). American Mineralogist, 91, 716.
Popp, R.K., Hibbert, H.A., and Lamb, W.M. (2006b) Oxy-amphbiole equilibria in Ti-bearing calic amphiboles: Experimental investigation and petrologic implications for mantle-derived amphiboles. American Mineralogist, 91, 54–66.
Schmid, R., Wilke, M., Oberhansli, R., Janssens, K., Falkenberg, G., Franz, L., and Gaab, A. (2003) Micro-XANES determination of ferric iron and its application in thermobarometry. Lithos, 70, 381–392.
Schumacher, J.C. (1991) Empirical ferric iron corrections—Necessity, assumptions, and effects on selected geothermobarometers. Mineralogical Magazine, 55, 3–18.
Simakov, S.K. (2006) Redox state of eclogites and peridotites from sub-cratonic upper mantle and a connection with diamond genesis. Contributions to Mineralogy and Petrology, 151, 282–296.
Wagner, C., Deloule, E., Fialin, M., and King, P.L. (2008) Dehydrogenation of kaersutitic amphibole under electron beam excitation recorded by changes in $Fe^{3+}/\Sigma Fe$: An EMP and SIMS study. American Mineralogist, 93, 1273–1281.
Williams, K.L. (1987) An Introduction to X-ray Spectrometry: X-ray fluorescence and electron microprobe analysis, xiii, 370 pp. Allen and Unwin, London.
Wood, B.J. and Virgo, D. (1989) Upper mantle oxidation state: Ferric iron contents of lherzolite spinels by ^{57}Fe Mossbauer spectroscopy and resultant oxygen fugacities. Geochimica et Cosmochimica Acta, 53, 1277–1291.
Wood, B.J., Bryndzia, L.T., and Johnson, K.E. (1990) Mantle oxidation-state and its relationship to tectonic environment and fluid speciation. Science, 248, 337–345.
Woodland, A.B., Kornprobst, J., and Tabit, A. (2006) Ferric iron in orogenic lherzolite massifs and controls of oxygen fugacity in the upper mantle. Lithos, 89, 222–241.

Manuscript received August 3, 2011
Manuscript accepted February 5, 2012
Manuscript handled by M. Darby Dyar